Yb:Ta:$RbTiOPO_4$, A New Strategy to Further Increase the Lanthanide Concentration in Crystals of the $KTiOPO_4$ Family

A. Peña, J. J. Carvajal, J. Massons, Jna. Gavaldà, F. Díaz, and M. Aguiló*

Física i Cristal·lografia de Materials (FiCMA), Universitat Rovira i Virgili (URV), Campus Sescelades c/ Marcel·lí Domingo, s/n E-43007 Tarragona, Spain

Received March 30, 2007. Revised Manuscript Received May 25, 2007

In this study, we determined the variation of the crystallization region of rubidium titanyl phosphate codoped with tantalum and yterbium at three different molar ratios of Rb_2O, P_2O_5, and TiO_2 in this ternary system. The amount of Yb^{3+} and Ta^{5+} that can substitute for Ti^{4+} without losing the desired phase strongly depends on the amount of TiO_2 in the initial solution. The critical amount of Yb^{3+} increases as the initial solution is richer in TiO_2. Yb:Ta:$RbTiOPO_4$ single crystals have been grown with dimensions and quality enough to perform their optic and spectroscopic characterization. The optical transparency window has been measured for $RbTi_{0.96}Ta_{0.04}OPO_4$ and $RbTi_{0.95}Ta_{0.03}Yb_{0.02}OPO_4$ crystals. Optical absorption and fluorescence of Yb^{3+} in $RbTi_{0.95}Ta_{0.03}Yb_{0.02}OPO_4$ have been recorded at room and low temperatures.

Introduction

$KTiOPO_4$ (KTP) and its isostructural $RbTiOPO_4$ (RTP) are well-known for their high nonlinear optical coefficients. Particularly KTP has been used as a frequency doubler of lasers emitting in the IR spectral range,[1,2] but this application can be extended as well to RTP.

One can assume that when doping with laser-active ions, such as lanthanide (Ln^{3+}) ions, these materials could be used as self-frequency doubling materials. It has been shown that the amount of Ln^{3+} ions with which KTP and RTP can be doped is too low to achieve efficient fluorescence.[3] However, by using a codopant such as Nb^{5+}, which expands the structure and acts as a charge compensator,[4] this amount increases until values high enough to obtain efficient fluorescence are obtained.[5,6] The presence of Nb^{5+} and Ln^{3+} ions with a concentration below 10 at % in RTP has been proven to have little dramatic effect on the NLO properties of the crystal or in the transparency range of the material.[7]

RTP belongs to a structural family with the general formula $ABOXO_4$, with A = K^+, Rb^+, Na^+, Cs^+, Tl^+, NH_4^+; B = Ti^{4+}, Sn^{4+}, Zr^{4+}, Ge^{4+}, V^{4+}; and X = P^{5+}, As^{5+}, which crystallizes in the orthorhombic system with the noncentrosymmetric space group $Pna2_1$ and $Z = 8$. The crystallization region of RTP in its self-flux and in tungstate fluxes has been previously determined.[8] The variation of this crystallization in the self-flux when introducing Nb^{5+} and Ln^{3+} (Er^{3+} and Yb^{3+}) has also been studied.[6] As it has been shown that the use of Nb^{5+} as a codopant enhances the distribution coefficients of lanthanide ions in the RTP matrix, the study of other possible codoping ions could be of interest to further increase the Ln^{3+} concentration.[6] A possible candidate is Ta^{5+}, which can be found in the same group of the periodic table than Nb^{5+} and, as well as this latter ion, has a slightly larger ionic radius ($r_{Ta^{5+}} = 0.640$ Å) than Ti^{4+} ($r_{Ti^{4+}} = 0.605$ Å)[9] and a larger ionic charge. In previous studies, it was shown that Ln^{3+} incorporation in crystals of the structural field of KTP increases when an element with a higher electronic charge and an ionic radius as close as possible to the ion to be substituted is used as codopant.[5] Ta^{5+} may then be a good choice for this purpose.

The Yb^{3+} ion has been chosen as the lanthanide active doping ion in this case, not only because its ionic radius is much closer to the Ti^{4+} than that of other Ln^{3+} ions but also because it is an ion with the same emission range as Nd^{3+}, at around 1 μm, having a much simpler energy level scheme, consisting of only two levels: the ground state ($^2F_{7/2}$) and the excited one ($^2F_{5/2}$). Some effects that lead to a reduction in the laser efficiency in other lanthanide ions, such as excited-state absorption, cross-relaxation, and up-conversion, are not present in this system. Furthermore, because of the closeness between the pumping and the laser wavelengths, there exists a small quantum defect that reduces the thermal loading of the crystals during laser operation. Moreover, the key point of doping RTP crystals (a noncentrosymmetric host) with Yb^{3+} is that Yb^{3+} has no absorption in the visible spectral range, the region in which self-frequency doubling laser action would take place, avoiding the absorption losses

* Corresponding author. E-mail: magdalena.aguilo@urv.cat.

(1) Zumsteg, F. C.; Bierlein, J. D.; Gier, T. E. *J. Appl. Phys.* **1976**, *47*, 4980.
(2) Jacco, J. C.; Loiacono, G. M. *Appl. Phys. Lett.* **1991**, *58*, 560.
(3) Rico, M.; Zaldo, C.; Massons, J.; Díaz, F. *J. Phys.: Condens. Matter* **1998**, *10*, 10101.
(4) Carvajal, J. J.; García-Muñoz, J. L.; Solé, R.; Gavaldà, Jna.; Massons, J.; Solans, X.; Díaz, F.; Aguiló, M. *Chem. Mater.* **2003**, *15*, 2338.
(5) Solé, R.; Nikolov, V.; Koseva, I.; Peshev, P.; Ruiz, X.; Zaldo, C.; Martín, M. J.; Aguiló, M.; Díaz, F. *Chem. Mater.* **1997**, *9*, 2745.
(6) Carvajal, J. J.; Nikolov, V.; Solé, R.; Gavaldà, Jna.; Massons, J.; Aguiló, M.; Díaz, F. *Chem. Mater.* **2002**, *14*, 3136.
(7) Carvajal, J.J.; Solé, R.; Gavaldà, Jna.; Massons, J.; Rico, M.; Zaldo, C.; Aguiló, M.; Díaz, F. *J. Alloys Compd.* **2001**, *323*−*324*, 231.
(8) Carvajal, J. J.; Nikolov, V.; Solé, R.; Gavaldà, Jna.; Massons, J.; Rico, M.; Zaldo, C.; Aguiló, M.; Díaz, F. *Chem. Mater.* **2000**, *12*, 3171.
(9) Shannon, R. D. *Acta Crystallogr., Sect. A* **1976**, *32*, 751.

10.1021/cm070887z CCC: $37.00
Published on Web 07/06/2007

for the generated second harmonic beam. Self-frequency doubling laser action has been achieved in some Yb^{3+}-doped noncentrosymmetric laser hosts, such as YCOB, GdCOB, MgO:LNB, and YAB with a Yb^{3+} concentration of $\sim 1 \times 10^{20}$ atoms/cm^{-3},[10] similar to that obtained in Yb:Nb:RTP crystals.[6] This, added to the recent achievement of IR laser operation in Yb:Nb:RTP crystals,[11] opens up the possibility to obtain self-frequency doubling laser action in the near future in these crystals, and consequently, if the conditions are favorable, also in Yb:Ta:RTP. However, obtaining self-frequency doubling laser action in these crystals is not trivial, as it can be achieved only by type II second harmonic generation (SHG) because of the region in which the original emission from Yb^{3+} ion is produced and the combination of refractive indexes implied in the frequency conversion. This contrasts with self-frequency doubling laser action obtained in other hosts, where type I SHG is the most usual frequency conversion used.

In this paper, we study the crystallization region of Yb:Ta:RTP and the amount of Yb^{3+} reached in each of the solution compositions studied. We have also performed some experiments of growth of Yb:Ta:RTP single crystals with which we have obtained crystals with the desired quality and size to undertake optic and further spectroscopic characterizations, such as room and low temperatures optical absorption and fluorescence. The efficiency of second harmonic generation in powdered samples of Ta:RTP and Yb:Ta:RTP has been evaluated with a KTP powdered sample as reference.

Experimental Section

Yb:Ta:RTP Crystallization Regions. Melt processes cannot be used to grow RTP single crystals and isostructurals because they melt incongruently and concretely at 1343 K in the case of RTP.[12] To begin the study, we chose three solution compositions with different ratios of precursor oxides, $Rb_2O-P_2O_5-(TiO_2 + Ta_2O_5 + Yb_2O_3) = 42.900-35.100-22.000$, $43.125-31.875-25.000$, and $40.800-27.200-32.000$. In every one of these solution compositions, we kept the ratio between Rb_2O and P_2O_5 constant and progressively substituted TiO_2 by Ta_2O_5 or Yb_2O_3 or by a combination of Ta_2O_5 and Yb_2O_3. In each case, we added Ta_2O_5 and Yb_2O_3 until the low-temperature orthorhombic phase of RTP disappeared. Rb_2CO_3 (99%), $NH_4H_2PO_4$ (99%), TiO_2 (99.9%), Ta_2O_5 (99.99%), and Yb_2O_3 (99.9%) were used as initial reagents to prepare the solutions. These reagents were mixed, placed in a 25 cm^3 Pt crucible, and heated until the total bubbling of NH_3, H_2O (coming from $NH_4H_2PO_4$), and CO_2 (coming from Rb_2CO_3) finished. The solutions, with a weight of 15−20 g, were homogenized in a vertical tubular furnace by keeping the temperature constant at around 75 K above the saturation temperature (T_s). To obtain the crystalline phase that crystallizes first as we decreased the temperature, we immersed a Pt wire inside the solution. The crucible was maintained at a position in which an axial gradient of almost 5 K/cm was produced, and we decreased the temperature at a rate of 10 K/h until the crystals nucleated and grew spontaneously on the Pt wire. We applied a slow cooling rate (3 K/h) to obtain a larger amount of small crystals to carry out phase identification by X-ray powder diffraction analysis. The morphological characterization of the as-grown crystals was performed using optical and scanning electron microscopes. Electron probe microanalysis (EPMA) was used to determine the dopant concentration as well as the atomic ratio between the chemical elements that compose the different crystalline phases. After the study of ~30 different solution compositions, the (Ta,Yb):RTP crystallization region in each of these three solution compositions was determined.

X-ray Powder Diffraction. X-ray powder diffraction was used to identify the different crystalline phases we found in the determination of the crystallization region of Yb:Ta:RTP. The characterization was performed in a Siemens D5000 powder diffractometer in a $\theta-\theta$ configuration using the Bragg−Brentano geometry. The diffraction patterns were recorded at $2\theta = 10-70°$, step size = 0.05°, and step time = 3 s.

Single-Crystal Growth. After the crystallization regions were determined, we chose one of those solution compositions, $Rb_2O-P_2O_5-(TiO_2 + Ta_2O_5 + Yb_2O_3) = 40.800-27.200-(29.000+1.000+2.000)$, to grow single crystals of Yb:Ta:RTP big enough for further characterizations, by using the top seeded solution growth−slow cooling (TSSG−SC) method. Crystals were grown in the same tubular furnace used for the determination of the crystallization regions, controlled by an Eurotherm 818P controller/programmer. The solution was prepared as explained before, with a weight of around 30 g and an axial gradient 4−10 K/cm, depending on the experience, adjusted to obtain good-optical-quality crystals, with the bottom of the crucible always hotter than the surface of the solution. All the crystal seeds used in the crystal growth process, except the first one, which was a single crystal of Ta:RTP obtained by spontaneous nucleation on a Pt wire, were of Yb:Ta:RTP composition. Crystal seeds were placed at the end of an aluminum rod with the *c* crystallographic direction perpendicular to the surface of the solution, and the *a* crystallographic direction radial to the rotation movement and centered with the rotation axis. The T_s value was determined accurately by controlling the growth or dissolution of the crystal seed in contact with the surface of the solution. The rotation was kept constant at 60 or 80 rpm during the crystal growth process. The change in the rotation speed was done to check the effect of the rotation on the quality of the crystals obtained. We decreased the temperature around 20 K from T_s at a cooling rate of 0.1 K/h. When the growth process was finished, we removed the crystal from the solution, keeping it over the surface of the solution while we cooled the furnace to room temperature at a cooling rate of 15 K/h.

Dopant Concentration Analyses. To measure the dopant concentrations in the samples, we analyzed Yb:Ta:RTP crystals by EPMA in a Cameca SX50 microprobe analyzer operating in the wavelength-dispersive mode. The sample preparation and the experimental procedure used to determine the concentration of all the different atoms is explained somewhere else.[13]

Second Harmonic Generation. We used the Kurtz method, a powder technique, to qualitatively determine the second harmonic generation (SHG) efficiency of Ta:RTP and Yb:Ta:RTP.[14] The experimental procedure was explained in a previous study.[8]

Transparency Window. In Ta:RTP and Yb:Ta:RTP crystals, we measured the transparency window between 300 and 9000 nm. Plate-shaped crystals perpendicular to the *a* direction and polished to optical quality were used. These plates came from a Ta:RTP crystal grown on a Pt wire and a Yb:Ta:RTP single crystal grown

(10) Brenier, A.; Jaque, D.; Majchrowski, A. *Opt. Mater.* **2005**, *28*, 310.
(11) Mateos, X.; Petrov, V.; Peña, A.; Carvajal, J. J.; Díaz, F.; Aguiló, M.; Segonds, P.; Boulanger, B. *Opt. Lett.* **2007**, in press.
(12) Cheng, L. K.; Bierlein, J. D.; Ballman, A. A. *J. Cryst. Growth* **1991**, *110*, 697.
(13) Carvajal, J. J.; Solé, R.; Gavaldà, Jna.; Massons, J.; Aguiló, M.; Diaz, F. *Cryst. Growth Des.* **2001**, *1*, 479.
(14) Kurtz, S. K.; Perry, T. T. *J. Appl. Phys.* **1968**, *39*, 3798.

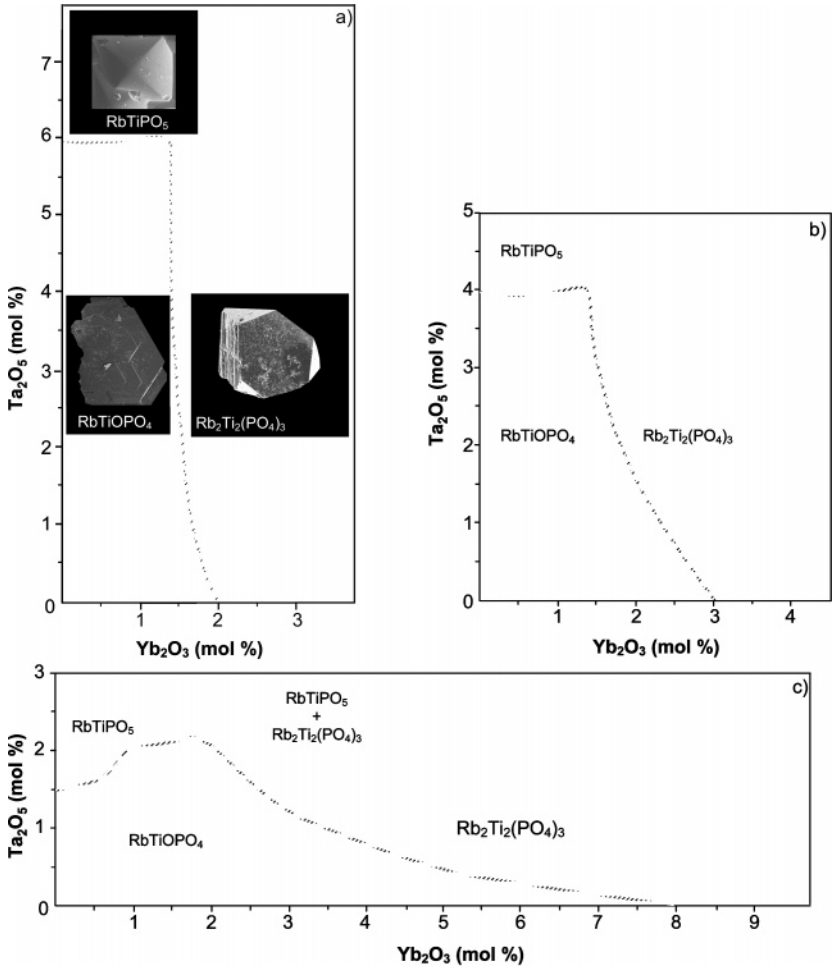

Figure 1. Evolution of the phase diagram of RTP, taking as basis the molar solution compositions of $Rb_2O-P_2O_5-(TiO_2 + Ta_2O_5 + Yb_2O_3)$ (a) 42.900−35.100−22.000, (b) 43.125−31.875−25.000, (c) 40.800−27.200−32.000, where we substituted progressively TiO_2 by Ta_2O_5 and Yb_2O_3, and SEM images of the crystalline phases identified are also shown.

by the TSSG−SC method. The two samples had a thickness of ~300 μm. The optical transparency of the crystals was measured using a Varian Cary 500 scan spectrophotometer in the range 300−3000 nm and using a FT-IR-680 Plus Fourier transformed infrared spectrometer in the range 3000−9000 nm.

Spectroscopic Characterization. The absorption spectra of Yb^{3+} in Yb:Ta:RTP crystals were measured at room and low temperatures using a Varian Cary 500 scan spectrophotometer in the 850−1100 nm range. Low temperatures were reached by using a Leybold RDK-6-320 closed-cycle cryostat. We used a Glan−Taylor polarizer to collect absorption spectra with light polarized along the three crystallographic axes.

Fluorescence measurements were performed by exciting the same sample used in the optical absorption studies, with a 200 mW diode laser emitting at $\lambda = 940$ nm, modulated at 1 kHz. The fluorescence spectra was recorded between 950 and 1100 nm at room and low temperatures in a 90° geometry, with the incident pumping beam in the *ab* plane and the detection recorded in the *bc* plane. The Yb^{3+} fluorescence was dispersed by a 460 mm monochromator (Jobin Ybon-Spex HR460) and detected by a cooled Hamamatsu NIR R5509-72 photomultiplier, which was connected to a lock-in amplifier. Low temperature, 10 K, was reached with a close-cycle cryostat (Oxford CCC1104).

Results and Discussion

Yb:Ta:RTP Crystallization Regions. We studied three solutions with three different molar ratios of $Rb_2O-P_2O_5-TiO_2$, in which we substituted TiO_2 by Ta_2O_5 or Yb_2O_3 or the two of them together and checked the amount of Yb^{3+} and Ta^{5+} allowed in the solution while maintaining the RTP phase, also called critical concentration. We also analyzed how the values of distribution coefficients, K_i, changed for Ti^{4+}, Ta^{5+}, and Yb^{3+}.

Figure 1 shows how the RTP crystallization region evolves as a function of the amount of dopants, Yb^{3+} and Ta^{5+}, in the solution. Figure 1a shows the RTP crystallization region in a solution containing 22 mol % TiO_2 and Rb_2O/P_2O_5 in a ratio of 1.2. Over a 6 at % Ta^{5+} solution, the high-temperature phase of RTP, $RbTiPO_5$,[15] crystallizes, and over 2 at % Yb^{3+} added to the initial solution, the phase which crystallizes is the langbenite, $Rb_2Ti_2(PO_4)_3$, phase.[16] The external morphologies of the three different phases are shown in SEM pictures in Figure 1a. The RTP phase shows a platelike habit similar to that obtained in Nb:RTP crystals,[17] whereas the two other phases show a more isometric habit. Figure 1b shows the Yb:Ta:RTP crystallization region for a

(15) Oseledchik, Y. S.; Belokrys, S. P.; Osadchuk, V. V.; Prosvirnin, A. L.; Selevich, A. F.; Starshenko, V. V.; Kuzemchenko, K. V. *J. Cryst. Growth* **1992**, *125*, 639.
(16) Carvajal, J. J.; Aznar, A.; Solé, R.; Gavaldà, Jna.; Massons, J.; Solans, X.; Aguiló, M.; Díaz, F. *Chem. Mater.* **2003**, *15*, 204.
(17) Carvajal, J. J.; Solé, R.; Gavaldà, Jna.; Massons, J.; Aguiló, M.; Díaz, F. *Cryst. Growth Des.* **2001**, *1*, 479.

Table 1. Distribution Coefficients of Ta^{5+} (K_{Ta}) and Yb^{3+} (K_{Yb}) for RTP Crystals Obtained in the Study of the Variation of the Crystallization Region of RTP When Codoping with Ta^{5+} and Yb^{3+} for Three Different Solution Compositions[a]

solution molar composition: $Rb_2O-P_2O_5-(TiO_2+Ta_2O_5+Yb_2O_3) = 42.900-35.100-22.000$			
	mol % Yb_2O_3 in solution		
mol % Ta_2O_5 in solution	0	1	2
2	RTP K_{Ta}= 1.91; K_{Yb}= 0.00	RTP K_{Ta}= 1.34 K_{Yb}= 0.16	RTP K_{Ta}= 1.45 K_{Yb}= 0.08; Rb_2
4	RTP K_{Ta}= 1.16; K_{Yb}= 0.00	RTP K_{Ta}= 1.09 K_{Yb}= 0.16	
6	RTP K_{Ta}= 0.80; K_{Yb}=0.00; Rb_5		

solution molar composition: $Rb_2O-P_2O_5-(TiO_2+Ta_2O_5+Yb_2O_3) = 43.125-31.875-25.000$		
	mol % Yb_2O_3 in solution	
mol % Ta_2O_5 in solution	**0**	**1**
2	RTP K_{Ta}= 1.96 K_{Yb}= 0.00	RTP K_{Ta}= 2.30 K_{Yb}= 0.31
4	RTP K_{Ta}= 0.96 K_{Yb}= 0.00	

solution molar composition: $Rb_2O-P_2O_5-(TiO_2+Ta_2O_5+Yb_2O_3) = 40.800-27.200-32.000$				
	mol % Yb_2O_3 in solution			
mol % Ta_2O_5 in solution	0	1	2	3
1	RTP K_{Ta}= 1.97; K_{Yb}= 0.00	RTP K_{Ta}= 1.81; K_{Yb}= 0.60	RTP K_{Ta}= 1.71; K_{Yb}= 0.45	RTP K_{Ta}= 1.43; K_{Yb}= 0.38
2	Rb_5	RTP K_{Ta}= 1.34; K_{Yb}= 0.45	RTP K_{Ta}= 1.96; K_{Yb}= 0.64; Rb_2	

[a] RTP = $RbTiOPO_4$; Rb_2 = $Rb_2Ti_{2-x}(Yb+Ta)_x(PO_4)_3$; Rb_5 = $RbTiPO_5$.

solution with a 1.4 Rb_2O/P_2O_5 ratio and 25 mol % TiO_2. In this case, the RTP high-temperature phase appeared beyond adding 4 at % Ta^{5+} in the initial solution and the maximum of Yb^{3+} allowed without losing the RTP phase is 3 at %: higher than this value, it appeared again as the langbeinite, $Rb_2Ti_2(PO_4)_3$, phase. Finally, Figure 1c shows the Yb:Ta:RTP crystallization region studied in a solution with a 1.5 Rb_2O/P_2O_5 ratio and a TiO_2 concentration of 32 mol %. The maximum concentrations of dopants that we can introduce in the solution while maintaining the RTP phase are 1.5 at % for Ta^{5+} and 8 at % for Yb^{3+}. So, one can see that for small values of the Rb_2O/P_2O_5 ratio and low concentrations of TiO_2, the critical concentration of Ta^{5+} in solution below which we can still grow the RTP phase reaches a value of 6 at %, the highest of the three molar ratios studied. On the other hand, the highest concentration of Yb^{3+} (8 at %) is reached for large values of the Rb_2O/P_2O_5 ratio and large concentrations of TiO_2.

The differences between the critical amount of Ta^{5+} and Yb^{3+} that are allowed in each crystallization region without losing the RTP phase can be explained in terms of the comparison between the ionic radii in an octahedral environment of Ti^{4+}, Ta^{5+}, and Yb^{3+}, as we expect Ta^{5+} and Yb^{3+} to substitute for Ti^{4+} in the crystalline structure, as with Yb:Nb:RTP crystals.[4] When the amount of Ta^{5+} increased, and because its distribution coefficient is always larger than unity, the solution composition that we get is richer in TiO_2 than the expected one. The quick incorporation of Ta^{5+} ($r_{Ta^{5+}}$ = 0.640 Å) in Ti^{4+} ($r_{Ti^{4+}}$ = 0.605 Å) sites was also observed in KTP.[18] Depending on the initial molar composition of the solution, the amount of codopant allowed could be larger or smaller. In the case of Yb^{3+} ($r_{Yb^{3+}}$ = 0.868 Å), because its distribution coefficient is always smaller than unity, the solution composition is poorer in TiO_2 than the expected one.

The neighboring phases that appeared in all cases were $RbTiPO_5$ and $Rb_2Ti_{2-x}(Yb+Ta)_x(PO_4)_3$. These phases were identified by X-ray powder diffraction and their stoichiometry was deduced from the results obtained by analyzing these crystals by electron probe microanalysis (EPMA). The diffraction patterns obtained were indexed according to the powder diffraction patterns of RTP, (entry 84-2356)[19] and $RbTiPO_5$ (entry 48-0016),[15] both in the database maintained by the Joint Committee for Powder Diffraction Standards (JCPDS), and that of $Rb_2Ti_2(PO_4)_3$.[16] When the amount of Ta_2O_5 in solution is increased, the $RbTiPO_5$ phase, belonging to the cubic system and with space group $Fd\bar{3}m$, crystallized.[15] When the critical concentration of Yb_2O_3 is reached, $Rb_2Ti_{2-x}(Yb+Ta)_x(PO_4)_3$ crystallizes, a langbeinite-type structure belonging to the cubic system and space group $P2_13$.[16]

Table 1 lists the distribution coefficients of Ta^{5+} and Yb^{3+} for the different crystals obtained in the study of the variation of the crystallization region of Yb:Ta:RTP depending on the

(18) Voronkova, V. I.; Yanovskiĭ, V. K.; Losevskaya, T. Yu.; Stefanovich, S. Yu.; Zverkov, S. A.; Alekseeva, O. A.; Sorokina, N. I. *Crystallogr. Rep.* **2004**, *49*, 123.
(19) Kaduk, J. A.; Jarman, R. H. *Z. Kristallogr.* **1993**, *204*, 285.

Table 2. Growth Data of the Crystals of (Yb,Ta):RTP, Using a Solution with a Composition $Rb_2O-P_2O_5-(TiO_2 + Ta_2O_5 + Yb_2O_3)$ = 40.800−27.200−(29.000+1.000+2.000) mol %, Obtained by the TSSG−SC Method

growth experiment	T_s (K)	seed width, *a* (mm)	rotation speed (rpm)	cooling program (cooling range (K)/cooling ramp (K/h))	crystal dimensions ($a \times b \times c$) (mm^3)	crystal weight (g)
1	1209.5		60	4/1 16.5/0.5	1.84 × 4.24 × 3.97	0.061
2	1208	1.84	60	4/1 27/0.2	2.46 × 8.47 × 7.09	0.339
3	1205	2.30	60	1/1 17.6/0.1	2.50 × 3.53 × 4.00	0.100
4	1207	3.00	80	1/1 20/0.1	3.19 × 5.73 × 5.50	0.182

initial solution composition. These distribution coefficients are defined as

$$K_B = \frac{([B]/[Ti] + [Ta] + [Yb])_{crystal}}{([B]/[Ti] + [Ta] + [Yb])_{solution}}$$

where B = Ti or Ta or Yb. The distribution coefficient K_{Ta}, is almost always larger than unity, but this value tends to decrease when the concentration of Ta^{5+} in the solution is increased. This has also been observed in KTP, where the Ta^{5+} concentration incorporated in the crystal is always higher than the expected when taking into account the Ta^{5+} concentration added in the initial solution.[18] Ta^{5+} ions are expected to replace Ti^{4+} ions in the structure. This could explain why K_{Ta} decreases when the Ta^{5+} concentration in the solution is increased, as the structure becomes saturated in Ta^{5+} and this ion cannot replace Ti^{4+} anymore. K_{Yb} always takes a value smaller than unity because Yb^{3+} has a larger ionic radius than Ti^{4+}. It can be seen in Table 1 that when the Rb_2O/P_2O_5 rate, the amount of TiO_2, and the amount of Ta_2O_5 in the initial solution increase, the value of K_{Yb} slightly increases until it reaches a maximum value of 0.64.

The values of K_{Yb} obtained may be explained in terms of (i) an expansion of the crystal structure due to the incorporation of Ta^{5+} ions that are slightly larger than Ti^{4+} ions, (ii) an expansion of the structure while crystallizing due to an increase in the saturation temperature when the amount of TiO_2 in solution is increased, and (iii) a decrease in the viscosity of the solution when there is a higher Rb_2O/P_2O_5 relation, which would lead to a better degree of homogenization of the solution, increasing the amount of Yb^{3+} ions that could enter into the structure of the growing crystal at the same time.

Top Seeded Solution Growth−Slow Xooling of Yb:Ta:RTP Crystals. Yb:Ta:RTP single crystals were grown by the TSSG−SC method in a solution with a composition $Rb_2O-P_2O_5-(TiO_2+Ta_2O_5+Yb_2O_3)$ = 40.800−27.200-(29.000+1.000+2.000). This composition is placed in the middle of the crystallization region shown in Figure 1c, in a point further from the border between the RTP and $Rb_2Ti_{2-x}(Yb+Ta)_x(PO_4)_3$ phases, which allowed it to obtain a larger concentration of Yb^{3+} in the crystals. The growth conditions are listed in Table 2. We studied how the changes in the speed of rotation, the cooling rate and the cooling interval affected the growth process.

Figure 2 shows a Yb:Ta:RTP crystal obtained following this procedure. In general, the crystals obtained have a flat morphology along the *a* direction. This morphology was previously observed in Nb:KTP[20] and Nb:RTP[13] single crystals. The crystals obtained tended to show some cracks along the *c* direction coming from the crystal seed. The crystals show the same faces as pure RTP: {100}, {011}, {201}, and {110}, listed from the most to the least developed, as can be seen in Figure 2. However, in Yb:Ta:RTP crystals, it should be noticed that the {100} face is much larger than the rest of the faces because the growth rate in the *a* direction is much slower than that in the *b* or *c* directions.To obtain more isometric crystals, we used wider crystal seeds, with dimensions between 1.8 and 3 mm, in the *a* direction, forcing crystal growth along this direction.

All crystal seeds used to grow Yb:Ta:RTP single crystals were placed centered in the rotation axis of the conical platinum crucible, with the wider dimension (the *a* crystallographic direction) in radial direction with respect to the rotation movement and the *c* crystallographic direction perpendicular to the solution surface.

The dimensions of the crystals obtained are listed in Table 2. These dimensions and the weight of the crystals obtained could be increased by enlarging the cooling interval during the growth process. However, the crystals obtained under these conditions had a low optical quality, with small crystals attached to their surface. This is due to spurious nucleation as the crystal that is growing is not able to absorb all the saturation that we are generating in the solution. So, to grow crystals with quality and size enough to carry out further characterizations, when the first additional crystal appears on the surface of the solution and nucleates spontaneously, we removed the main crystal from the solution and decreased the temperature to room temperature before taking the crystal from the furnace. A concentration of Yb^{3+} of 1.6×10^{20} atoms/cm^3 has been obtained in these crystals.

Second Harmonic Generation. The efficiency of the second harmonic generation process, defined as the ratio between the power of the reflected pumping beam generated by a Nd:YAG laser (λ = 1064 nm) and the doubled one generated by the sample (λ = 532 nm), has been measured in RTP samples doped only with Ta^{5+} and in RTP samples doped with Ta^{5+} and Yb^{3+}. The SHG efficiency of a $RbTi_{0.96}Ta_{0.04}OPO_4$ crystal compared to that of KTP is $\eta_{Ta:RTP}/\eta_{KTP}$ = 0.95. For a sample of $RbTi_{0.95}Ta_{0.03}Yb_{0.02}OPO_4$, the efficiency decreases some ($\eta_{(Ta,Yb:RTP)}/\eta_{KTP}$ = 0.80), but the presence of Yb^{3+} in the crystals has a nondramatic effect on the SHG efficiency. This decrease in the efficiency of the second harmonic generation process could be due to a smaller distortion in the TiO_6 octahedra, as proposed by Hagerman

(20) Wang, J.; Liu, Y.; Wei, J.; Jiang, M.; Shao, Z.; Liu, W.; Jiang, S. *Cryst. Res. Technol.* **1997**, *32*, 319.

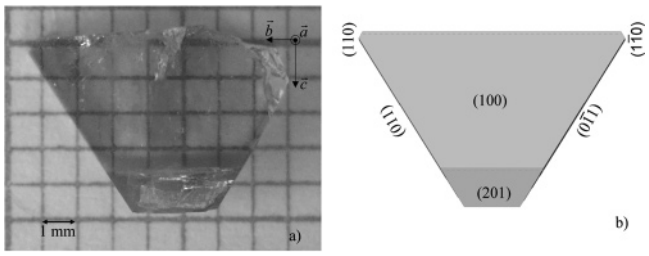

Figure 2. (a) $RbTi_{0.95}Ta_{0.03}Yb_{0.02}OPO_4$ single-crystal grown by the TSSG−SC method on a *c* oriented crystalline seed and (b) scheme of its morphology with the Miller indices of the different faces that appear in the crystal.

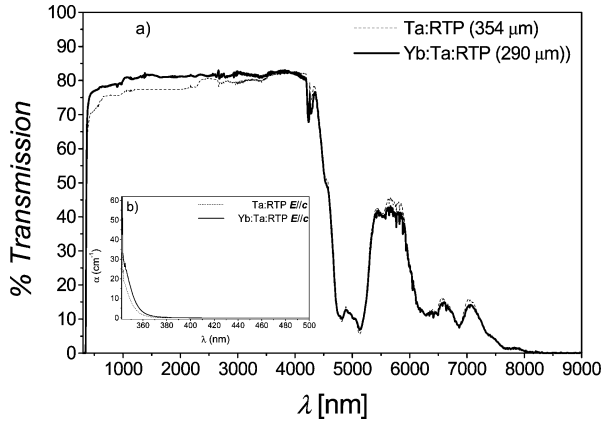

Figure 3. (a) Optical transparency window of $RbTi_{0.96}Ta_{0.04}OPO_4$ (dashed line) and $RbTi_{0.95}Ta_{0.03}Yb_{0.02}OPO_4$ (solid lines) single crystals. (b) Evolution of the cutoff value in the UV region for these crystals.

et al.,[21] or to a decrease in the ionicity in the interactions of the cation framework, as proposed by the extension of the ionic model of second-order susceptibility (χ_{ijk}^2) by Phillips et al.[22] However, no studies on these directions have been performed for the moment in these crystals.

Transparency Window. We have determined the UV and the IR cutoff wavelengths that close the optical transparency window in Ta:RTP and Yb:Ta:RTP samples (Figure 3). The wavelength of the UV cutoff is taken when the optical transmission decays for a factor of 1/*e*. For Ta:RTP crystals, with a thickness of 350 μm, the UV cutoff value is located at 340 nm and the IR cutoff is located at ∼7500 nm. Similar cutoff wavelengths have been obtained for a Yb:Ta:RTP crystal with a thickness of 290 μm, with the UV cutoff wavelength being located at 342 nm.

It has been previously said that by doping KTP, there exists an enhancement of the susceptibility to optical damage, related to the growth of optical absorption bands close to the UV cutoff.[23,24] We collected the optical absorption of $RbTi_{0.96}Ta_{0.04}OPO_4$ at room temperature in the 350−500 nm range using polarized light parallel to the *c* crystallographic direction and it appears as a band centered around 595 nm, which is similar to those observed in damage or reduced KTP samples.[25] This band is related to the overlapping contribution of $^2T_2 \rightarrow {}^2E$ transition of Ti^{3+} in Ti(1) and Ti(2) sites of the RTP lattice and disappears after the crystals are annealed at around 800 K for 5 h. If we compare the values obtained for the UV cutoff with those previously reported for $RbTiOPO_4$ (342 nm) and $RbTi_{0.94}Nb_{0.06}OPO_4$ (350 nm),[17] using polarized light parallel to the *c* crystallographic direction, it seems that the UV cutoff of $RbTi_{0.96}Ta_{0.04}OPO_4$ (344 nm) has been red-shifted with respect to that of $RbTiOPO_4$.

This UV cutoff is due to Ti−O electronic transitions, and its value depends on whether tantalum octahedra or only titanium octahedra are present in the structure. As we already know that the UV cutoff for $KTaO_3$ is 365 nm and that by substituting Ta^{5+} by Nb^{5+} in the structure this value increases until 385 nm,[26] the results obtained in our work are in agreement with those previously reported, which is that the cutoff wavelength is smaller in RTP than in Ta:RTP and Nb:RTP.[17]

The bands and peaks that appear in the IR region of the optical transparency window, shown in Figure 3 and centered between 2600 and 2800 nm, are due to the presence of OH^- groups. All the other bands in the spectra between 3300 nm until the end of the spectra (around 8 μm) are combination and overtone bands of the vibrational modes of PO_4^{3-}. The broad and weak band centered at 3400 nm is due to the second overtone of the ν_3, the broad and intense band between 4000 and 5200 nm is the first overtone of ν_3, and the small band at around 5520 nm can be attributed to the first overtone of ν_1. At 6300 nm, the combination band ($\nu_3 + \nu_4$) appears, and at 7500 nm, the band that closes the optical transparency window in the IR region, which corresponds to the combination band ($\nu_1 + \nu_2$), appears. The obtained spectrum is close to that previously obtained by Jacco et al.[2] for KTP, and the bands' assignments have been done with the help of previously published studies.[2,27]

In the spectra of the $RbTi_{0.95}Ta_{0.03}Yb_{0.02}OPO_4$ crystal, the band between 900 and 990 nm corresponds to the Yb^{3+} absorption band associated with the $^2F_{7/2} \rightarrow {}^2F_{5/2}$ transition of Yb^{3+}, which will be studied in more depth in the next section.

Spectroscopic Characterization. We characterized the Yb^{3+} ion in Yb:Ta:RTP crystals spectroscopically. All three possible polarization configurations were studied. The intensity of the spectrum collected with incident light polarized parallel to the *a* axis is much lower than the intensity of the spectrum collected with incident light polarized parallel to the other two axes, showing the same shape of the spectrum collected with light polarized parallel to the *b* direction. To record the spectra in $RbTi_{0.95}Ta_{0.03}Yb_{0.02}OPO_4$, we used a small cube ($1.64 \times 1.63 \times 1.81$ mm^3), obtained from the crystal shown in Figure 2. The optical absorption spectra were recorded at room temperature (Figure 4a) with the incident light polarized parallel to the *a*, *b*, and *c* crystallographic axes.

(21) Hagerman, M. E.; Poeppelmeier, K. R. *Chem. Mater.* **1995**, *7*, 602.
(22) Phillips, M. L. F.; Harrison, W. T. A.; Gier, T. E.; Stucky, G. D.; Kulkarni, G. V.; Burdett, J. K. *Inorg. Chem.* **1990**, *29*, 2158.
(23) Martín, M. J.; Zaldo, C.; Díaz, F.; Solé, R.; Bravo, D.; López, F. J. *Radiat. Eff. Defects Solids* **1995**, *136*, 243.
(24) Zaldo, C.; Carvajal, J.; Solé, R.; Díaz, F.; Bravo, D.; Kling, A. *J. Appl. Phys.* **2000**, *88*, 3242.
(25) Martín, M. J.; Bravo, D.; Solé, R.; Díaz, F.; López, F. J.; Zaldo, C. *J. Appl. Phys.* **1994**, *76*, 7510.
(26) Wang, X.; Wang, J.; Yu, Y.; Boughton, R. I. *J. Cryst. Growth* **2006**, *293*, 398.
(27) Vivekanandan, K.; Selvasekarapandian, S.; Kolandaivel, P.; Sebastian, M. T.; Suma, S. *Mater. Chem. Phys.* **1997**, *49*, 204.

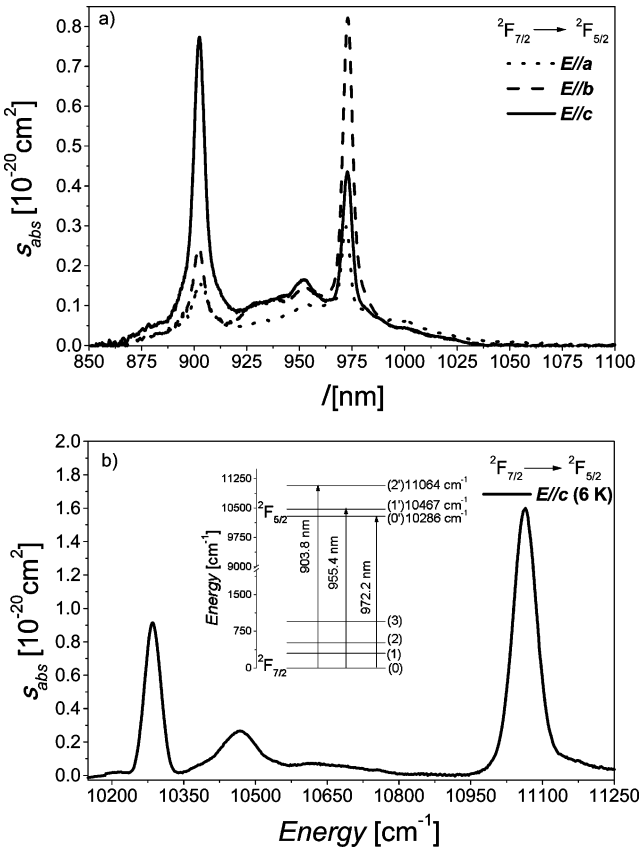

Figure 4. (a) Polarized absorption spectra of the $^2F_{7/2} \rightarrow {}^2F_{5/2}$ transition at room temperature with light polarized parallel to the *a* (dotted line), *b* (dashed line), and *c* (solid line) crystallographic axes in a $RbTi_{0.95}Ta_{0.03}Yb_{0.02}OPO_4$ single crystal, and (b) low-temperature spectrum recorded with light parallel to the *c* crystallographic axis.

The recorded absorption spectra (Figure 4a) show dichroism: when the light is polarized parallel to the *c* crystallographic axis, the most intense peak is located at 903.8 nm, and when it is polarized parallel to the *a* and *b* crystallographic axes, the most intense peak is found at 972.2 nm. The intensity of the peaks as a function of the polarization of the light may vary, but the position or number of peaks are independent of the polarization of the light, as Yb^{3+} has an odd number of electrons in the 4f shell, and then no selection rules exist for the induced electric dipole. The three peaks that appeared in the low-temperature spectra (recorded with light polarized parallel to the *c* axis and shown in Figure 4b) are due to electronic transitions between the ground state ($^2F_{7/2}$) and the three Stark levels of the excited state ($^2F_{5/2}$).

The unpolarized fluorescence spectrum was recorded at room and low temperatures with the same cube used to record the absorption spectra, on a $RbTi_{0.95}Ta_{0.03}Yb_{0.02}OPO_4$ single crystal. The spectrum obtained (see Figure 5), shows four peaks in the low-temperature spectra, and five peaks in the room-temperature spectra, corresponding to the emission from the excited state $^2F_{5/2}$ to the $^2F_{7/2}$ ground state. The most intense peak is centered at 972.2 nm, and it determines the energy of the $^2F_{5/2}(0')$ sublevel because this peak corresponds to the $^2F_{5/2}(0') \rightarrow {}^2F_{7/2}(0)$ electronic transition. A broad band was observed between 1001.7 nm ($^2F_{5/2}(0') \rightarrow {}^2F_{7/2}(1)$) and 1023.2 nm ($^2F_{5/2}(0') \rightarrow {}^2F_{7/2}(2)$). Finally two other peaks of

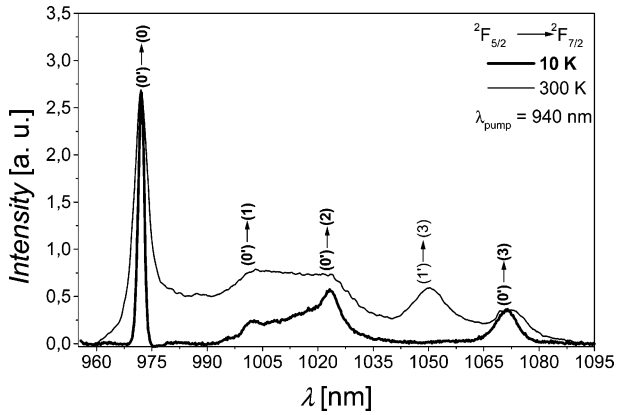

Figure 5. Unpolarized photoluminescence at room and low temperatures of the $^2F_{5/2} \rightarrow {}^2F_{7/2}$ transition for a $RbTi_{0.95}Ta_{0.03}Yb_{0.02}OPO_4$ single crystal after optical pumping at 940 nm with a diode laser.

lower intensity were observed at 1051.1 nm ($^2F_{5/2}(1') \rightarrow {}^2F_{7/2}(3)$) (observed only in the room-temperature spectra) and 1071.5 nm ($^2F_{5/2}(0') \rightarrow {}^2F_{7/2}(3)$).

Both absorption and emission spectra obtained for Yb:Ta:RTP crystals match well, in shape and in position of the peaks with the spectra previously obtained for Yb:Nb:RTP crystals,[28] showing only a slight blue-shift of the peaks in Yb:Ta:RTP crystals. This is important because a broad laser emission around 1 μm can also be obtained in these crystals that may allow for the generation of ultrashort laser pulses and the development of new tunable laser sources.[25]

Conclusions

We obtained Yb:Ta:RTP single crystals doped with enough concentration of Yb^{3+} to get efficient fluorescence at room temperature. When comparing with RTP single crystals codoped with Nb^{5+} and Yb^{3+}, it is interesting to note that using a smaller concentration of Ta^{5+}, instead of Nb^{5+}, in a solution with the same molar composition of precursor oxides, Rb_2O, P_2O_5, and TiO_2, the concentration of Yb^{3+} reached is higher. This is important, as by introducing fewer impurities in the crystal, we get the same Yb^{3+} concentration in the host, minimizing changes in the physical properties of these crystals caused by the presence, at larger concentrations, of these impurities. However, the crystallization region of RTP when using Ta^{5+} as a codopant is much narrower than the crystallization region obtained when using Nb^{5+}. The critical concentration of Ta^{5+} and Yb^{3+} depends on the initial solution composition and the molar concentration of Rb_2O, P_2O_5, and TiO_2. The boundary phases to RTP in these systems are $RbTiPO_5$ above the critical concentration of Ta^{5+}, and $Rb_2Ti_{2-x}(Yb + Ta)_x(PO_4)_3$ above the critical concentration of Yb^{3+}. Spectroscopic studies revealed a strong dichroism that can be useful to optimize the fluorescence response by pumping at different wavelengths for different polarization configurations of the incident light, at around 903 nm when the incident light is polarized along the *c* crystallographic axis, or 973 nm when the incident light is polarized along the *b* crystallographic axis. The same

(28) Carvajal, J. J.; Solé, R.; Gavaldà, Jna.; Massons, J.; Segonds, P.; Boulanger, B.; Brenier, A.; Boulon, G.; Zaccaro, J.; Aguiló, M.; Díaz, F. *Opt. Mater.* **2004**, *26*, 313.

behavior was shown in Yb:Nb:RTP. Also, by comparing the absorption and emission spectra of Yb:Ta:RTP crystals with those obtained on Yb:Nb:RTP crystals,[28] we expect that Yb^{3+} in Yb:Ta:RTP crystals emits with a broad laser emission band at around 1 μm, useful for the generation of ultrashort laser pulses and the development of new tunable laser sources.[11]

Moreover, because of the high SHG process efficiency, even when Yb^{3+} is present in the crystals, Yb:Ta:RTP is a good candidate to be tested as a self-frequency doubling material.

Acknowledgment. This work has been supported by the Spanish government under projects MAT-05-06354-C03-02, MAT-04-20471-E, and CIT-020400-2005-14 and the Catalan government under project 2005SGR658. A.P. thanks to the Spanish government for the personal funding BES-2003-1694.

CM070887Z